

Investigations of Flow Field with Different Turbulence Models on NREL Phase VI Blade

T. Y. Liu, C. H. Lin., Y. M. Ferng

Abstract—Wind energy is one of the clean renewable energy. However, the low frequency (20-200HZ) noise generated from the wind turbine blades, which bothers the residents, becomes the major problem to be developed. It is useful for predicting the aerodynamic noise by flow field and pressure distribution analysis on the wind turbine blades. Therefore, the main objective of this study is to use different turbulence models to analyze the flow field and pressure distributions of the wing blades.

Three-dimensional Computation Fluid Dynamics (CFD) simulation of the flow field was used to calculate the flow phenomena for the National Renewable Energy Laboratory (NREL) Phase VI horizontal axis wind turbine rotor. Two different flow cases with different wind speeds were investigated: 7m/s with 72rpm and 15m/s with 72rpm.

Four kinds of RANS-based turbulence models, Standard k- ϵ , Realizable k- ϵ , SST k- ω , and v2f, were used to predict and analyze the results in the present work. The results show that the predictions on pressure distributions with SST k- ω and v2f turbulence models have good agreements with experimental data.

Keywords—Horizontal Axis Wind Turbine, turbulence model, noise.

I. INTRODUCTION

THE reserve of fossil fuel is limited presently in the world and the chemical materials discharged, due to combustion, would result in environmental pollution and greenhouse effect and can be seen everywhere. These influences would cause serious impact on the natural environment and ecosystem. In addition, the problem around the lack of indigenous energy in Taiwan has existed all the time, in which 98% energy rely heavily on imported energy products. Developing clean energy is very important, therefore, gradually significant issue. With respect to the topography and renewable energies in Taiwan, the islands district would be affected by monsoons all the whole year, hence wind power is an extremely potential renewable energy. In terms of Taiwan with high urban density, small-scale wind power turbine is more suitable for the home-environment districts and provides the electric power requirement for residential areas. However, the low frequency noise generated from the wind turbine blades becomes the major problem, especially for bothering the residents.

Lighthill [1] provided an acoustic wave equation derived from fluid dynamics theory in 1952. The acoustic field is obtained from the experimental data or Computational Fluid Dynamic (CFD). This kind of the approach, which segregates the calculations of the flow and acoustic fields, is called

acoustic analogy. Subsequently, Ffowcs Williams and Hawking [2] derived the Navier-Stokes equations based on acoustic analogy theory and consider the coupling influence between solid wall and acoustic. Then, Ffowcs Williams-Hawking (FW-H) equation was derived and an effective tool for the noise problem.

The analysis of flow field is quite significant for accuracy before predicting noise problem. Most of researches on flow field employed Large Eddy Simulation (LES) to predict the flow characteristics. However, the computational resources are quite huge and time consuming. Therefore, it is important for using different turbulence models to analyze the flow characteristics accurately. In the present work, the simulation of wind blade based on NREL Phase VI [3] was performed to make comparisons with the results from experimental data [4] under different turbulence models. Further, the prediction of the acoustic field can be estimated the influence by the suitable turbulence model

II. MATHEMATICAL MODELS

Simulating the phenomena of fluid flowing through the wind blade has to meet mass and momentum conservation laws. The assumptions of the modeling are three-dimensional model, incompressible flow, neglect of the gravity influence, fluid properties without change by temperature, etc. In addition, the wall of the wind blade is smooth and satisfies no-slip condition. The governing equations are as followed.

Mass Equation

$$\nabla \cdot (\rho \mathbf{u}) = 0 \quad (1)$$

Momentum Equation

$$\frac{\partial(\rho \bar{\mathbf{u}})}{\partial t} + \nabla \cdot (\rho \bar{\mathbf{u}} \bar{\mathbf{u}}) = -\nabla P + \nabla \cdot (\mu \nabla \bar{\mathbf{u}}) \quad (2)$$

where p is pressure and μ is fluid viscosity.

Turbulence Models

The turbulent phenomenon is quite complex and difficult to present the complete flow characteristics. At present, LES model has good agreement with measurement and observation on flow field. However, LES model needs not only huge computational resources and time, but also finer meshes to perform. Therefore, an appropriate turbulence model for accurately predicting the experimental data, meshes design and suitable boundary conditions are quite significant issues. In the present work, four RANS-based turbulence models, Standard

T.Y. Liu is with the National Tsing Hua University, Taiwan (phone: 035510890; e-mail: smallayoyo@gmail.com).

C.H Lin and Y.M Ferng are with National Tsing Hua University, Taiwan (e-mail: gp6ej3@gmail.com, ymfeng@ess.nthu.edu.tw).

k- ϵ 、Realizable k- ϵ 、SST k- ω 、 $v2f$, were employed to predict the flow field under normal operation of wind turbine. The equations around the four turbulence models are presented as below.

Turbulent Kinetic Equation (K)

$$\frac{\partial}{\partial t}(\rho k) + \frac{\partial}{\partial x_i}(\rho k u_i) = \frac{\partial}{\partial x_j} \left[\left(\mu + \frac{\mu_t}{\sigma_k} \right) \frac{\partial k}{\partial x_j} \right] + G_k + G_b + -\rho \epsilon - Y_M + S_k \quad (3)$$

Turbulent Dissipation Equation (ϵ)

$$\frac{\partial}{\partial t}(\rho \epsilon) + \frac{\partial}{\partial x_i}(\rho \epsilon u_i) = \frac{\partial}{\partial x_j} \left[\left(\mu + \frac{\mu_t}{\sigma_\epsilon} \right) \frac{\partial \epsilon}{\partial x_j} \right] + C_{1\epsilon} \frac{\epsilon}{k} + (G_k + G_{3\epsilon} G_b) - C_{2\epsilon} \rho \frac{\epsilon^2}{k} + S_\epsilon \quad (4)$$

Specific Dissipation Rate (ω)

$$\frac{\partial}{\partial t}(\rho \omega) + \frac{\partial}{\partial x_i}(\rho \omega u_i) = \frac{\partial}{\partial x_j} \left[\Gamma_\omega \frac{\partial \omega}{\partial x_j} \right] + G_\omega - Y_\omega + D_\omega + S_\omega \quad (5)$$

III. MODELING DESCRIPTIONS

Turbulence model is an important mechanism on predicting pressure distribution on wind blade for analyzing the acoustic field. The analysis of different turbulence models can be used to understand what turbulence model is the appropriate one to predict the flow characteristics and pressure distribution effectively. Therefore, verification of turbulence models plays an important role initially in the present work.

The experimental data for a wind blade is presented by NREL Phase VI [4], as shown in Fig. 1. The tip of the wind blade is the model of NREL S809, and the bottom is a cylinder connected on the nacelle. The bottom part is located at 30% twist angle and the chord length is 5.029 m, in which the shape of the tip is assumed as a flat surface, as presented in Fig. 2. The nacelle and the tower structure were neglected [5]. Fig. 3 shows the illustration of the wind blades and the surrounding domain. With respect to the meshes distribution, the wall of the wind blade and its adjacent zone set the finer meshes, due to the existence of separation flow and rotation effect between fluid and blades, especially for a specific problem around stagnation occurring on the upwind surface. For the far-field zone, the coarser meshes can be employed to reduce computational time. The definition of the far-field domain was set as a cylinder of 12m diameter. The height of the wind blades was 12.192m. The zone of the rotor, rotating with the wind blades, was set as a cylinder with a radius of 6 m and a height of 1.5m. The wind blades were designed as two-blade wind turbine and the rotation speed was 72rpm with two types of wind speeds, as shown in Table I.

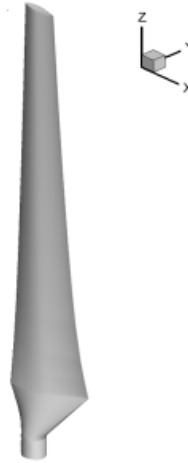


Fig. 1 The model of the NREL Phase VI

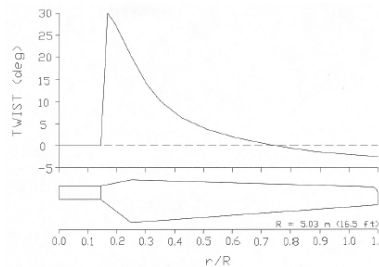


Fig. 2 The distribution of the twist angle for the NREL Phase VI

TABLE I
OPERATION CONDITIONS FOR TWO CASES

Profile of wind blade	NREL S809
Wind speed (m/s)	7,15
Rotation speed (rpm)	72
Mesh number	5814235
Case 1	Wind speed : 7m/s
Case 2	Wind speed : 15m/s

Mesh sensitivity tests is an important work to ensure the reduction of the numerical errors initially. Two kinds of meshes designs, 2,105,622 and 5,814,235, were performed to compare with the experimental data of the coefficient of pressure (C_p) [4], respectively, as presented in Fig. 4. Structured grids were employed on near the wall for controlling the quality and quantity of meshes effectively. Unstructured grids were used on far-field zone. Fig. 5 shows the computational results using standard k- ϵ turbulence model for the C_p in comparison with the experimental data [4]. The abscissa is the ratio of the wind blade location. Herein, x/c means the fore part of the wind blade and $x/c = 1$ means the tail part. The ordinate is the C_p . For comparing with the experimental data, the computational result with finer meshes (5,814,235) design shows that the fore part of the wind blade has good agreement. In addition, the variation in C_p is not obvious between using standard k- ϵ turbulence model and experience data, except for predicting the fore part of the wind blade. The main difference between experience data and turbulence models used in this work would be discussed as

below. In order to predict accurately, the finer meshes (5,814,235) design would be, therefore, employed for further studies.

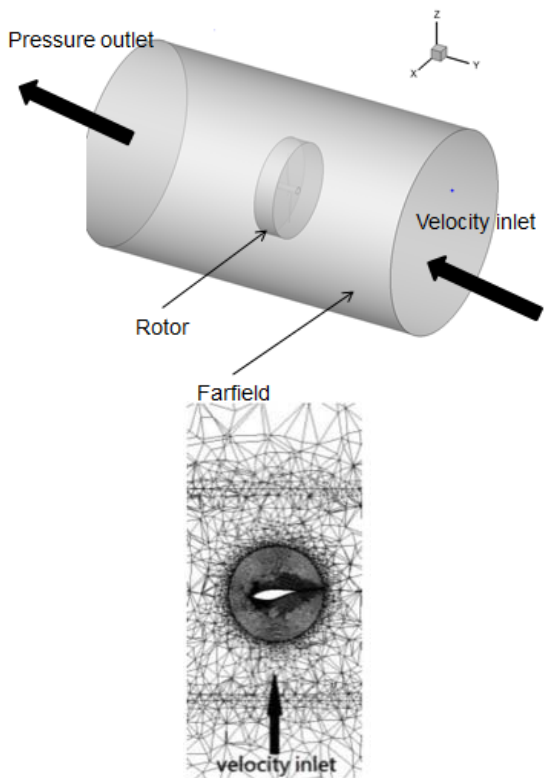


Fig. 3 The computational domain

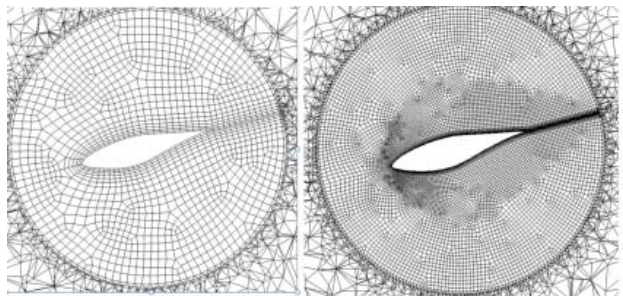


Fig. 4 Two kinds of Mesh distributions

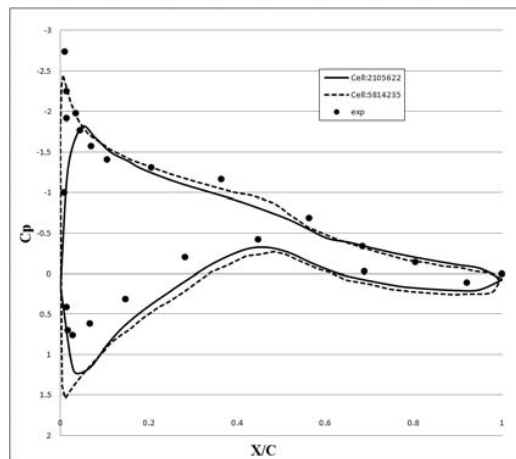


Fig. 5 The mesh sensitivity tests

IV. RESULTS AND DISCUSSIONS

Fig. 6 shows that the C_p distribution at the relative height of 30% for case 1. The values of C_p with Standard $k-\epsilon$ turbulence model are obviously larger than other turbulence models. This means the static pressure is larger and the relative velocity is lower than those calculated with other turbulence models. The trend is in accordance with the relative velocity distribution. The simulation results with SST $k-\omega$ and $v2f$ turbulence models have good agreements with experimental data. In addition, the C_p distribution with Realizable $k-\epsilon$ turbulence model obviously overestimates at the fore part of the wind blade in comparison with the experimental data.

The same trends for the simulations with Realizable $k-\epsilon$ turbulence model occur in Figs. 7 and 8. This overestimated distribution at the fore part of the wind blade would more obvious as the wind speed is lower. The main reason is that the Realizable $k-\epsilon$ turbulence model includes the effects of mean rotation in the definition of the turbulent viscosity. The extra rotation effect has better simulation results on single rotating frame system. However, the computational domain of wind blades and rotor includes both rotating and stationary fluid zones. The result would produce non-physical turbulent viscosities in this situation due to the modification of Realizable $k-\epsilon$ turbulence model. Therefore, Realizable $k-\epsilon$ turbulence model is not appropriate for the prediction of wind blades system. For SST $k-\omega$ and $v2f$ turbulence models, the predictions on C_p distributions have good agreements with experimental data.

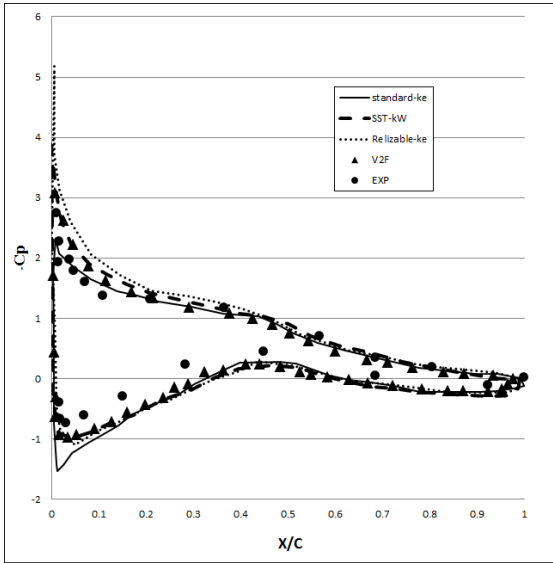


Fig. 6 The Cp distribution at the relative height of 30% for case 1

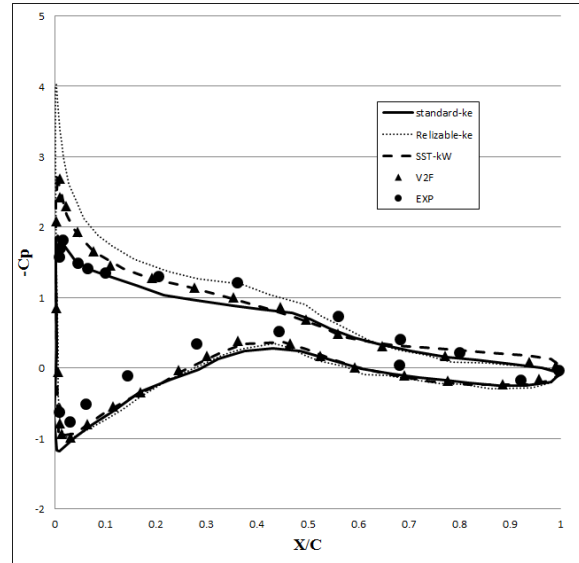


Fig. 8 The Cp distribution at the relative height of 80% for case 1

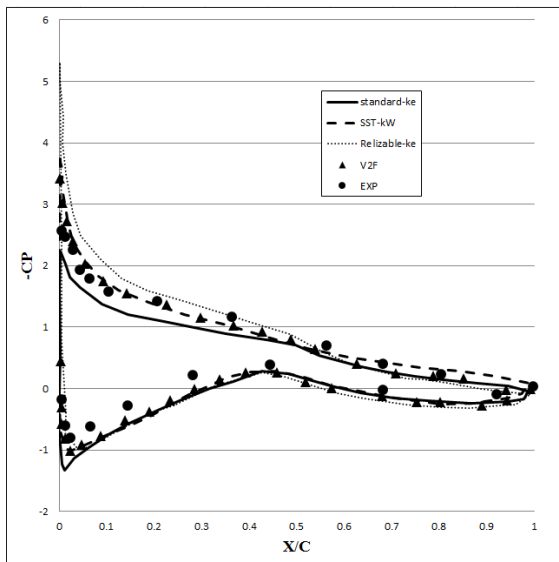


Fig. 7 The Cp distribution at the relative height of 47% for case 1

Fig. 9 shows that the Cp distribution at the relative height of 30% for case 2. For the simulation results with Standard k-ε turbulence model, the whole trend is similar to the experience data, except for the wake zone. For Realizable k-ε turbulence model, the unreasonable phenomenon occurring at the fore part of the wind blade would more obvious. The main reason is still that the effects of mean rotation in the definition of the turbulent viscosity are included in the Realizable k-ε turbulence model. The computational domain includes both rotating and stationary fluid zones. The non-physical phenomenon will happen, therefore, occur at the fore part of the wind blade. The predictions with SST k-ω and v2f turbulence models also have good agreement on that with experience data. These two turbulence models could effectively capture the flow characteristics at the wake zone. Figs. 10 and 11 present that the Cp distribution at the relative height of 47% and 80% for case 2, respectively. The predictions with SST k-ω and v2f turbulence models have good agreement with experimental data.

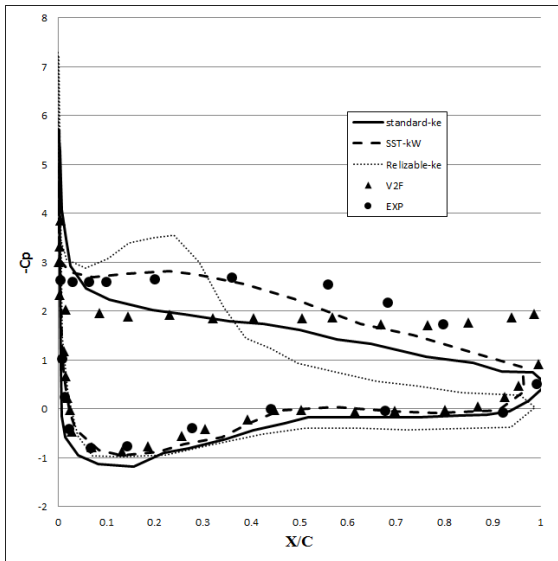


Fig. 9 The Cp distribution at the relative height of 30% for case 2

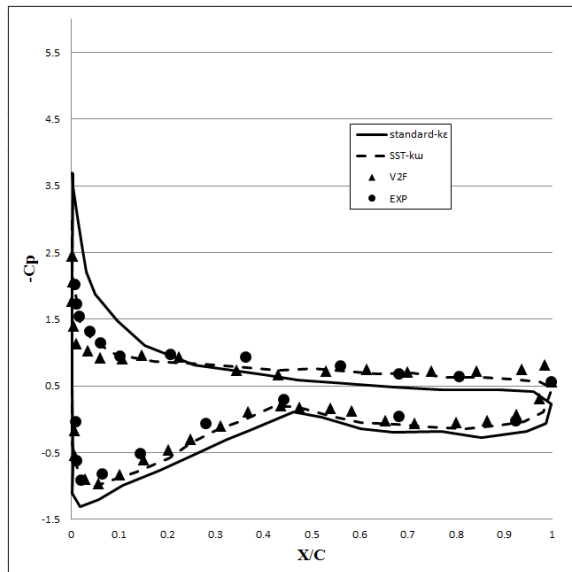


Fig. 11 The Cp distribution at the relative height of 80% for case 2

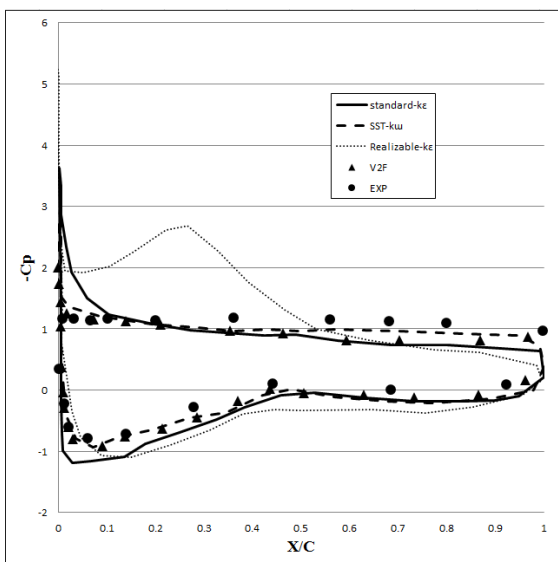


Fig. 10 The Cp distribution at the relative height of 47% for case 2

V. CONCLUSION

Three-dimensional CFD simulation with different turbulence models was employed to calculate the flow field and pressure distributions on NREL Phase VI wind turbine in this study. Most of investigations on flow field of wind blades using LES turbulence model to predict the flow characteristics. However, the computational resources are quite huge and time consuming. Therefore, it is very important for using different turbulence models to analyze the flow characteristics accurately. In comparison with the experimental data for case 1, the predictions with four RANS-based turbulence models have good agreements with experiments. The distributions of flow field with these turbulence models have few variations in comparison with that with experience data. With wind speed increasing, the simulations with RANS-based turbulence models gradually form obvious variations, especially for flow field distribution with Realizable $k-\epsilon$ turbulence model at the wake zone. The main reason is that the Realizable $k-\epsilon$ turbulence model includes the effects of mean rotation in the definition of the turbulent viscosity. However, the computational domain of wind blades and rotor includes both rotating and stationary fluid zones. The result would result in non-physical turbulent phenomenon. Therefore, Realizable $k-\epsilon$ turbulence model is not appropriate for the prediction of wind blades system.

LES turbulence model can capture effectively this phenomenon at the wake flow. However, the objective of this study is mainly to focus on the pressure distribution on the wind blades. The influence of the noise is affected by the pressure distribution. Therefore, accurate prediction on pressure distribution is the main purpose in the present work. The predictions with SST $k-\omega$ and v2f turbulence models have good agreement on that with LES turbulence model. These two turbulence models could effectively capture the flow characteristics at the wake zone. Furthermore, the calculations

of flow field using SST $k-\omega$ and $v2f$ turbulence models not only have good agreements with that using LES turbulence model, but also are in accordance with the experimental data on C_p distributions.

REFERENCES

- [1] M.J. Lighthill, "On Sound Generated Aerodynamically. I. General Theory," Proceedings of the Royal Society of London Series A, Mathematical and Physical Sciences, Vol. 211, 1952, 564-587.
- [2] J. E. Ffowcs Williams and D. L. Hawkins, "Sound Generation by Turbulence and Surfaces in Arbitrary Motion," Philosophical Transactions of Royal Society of London, Series A, Mathematical and Physical Sciences, Vol. 264, 1964, 321-342.
- [3] Giguere, P. and Selig, M. S., "Design of a Tapered and Twisted Blade for the NREL Combined Experiment Rotor," Nrel/sr-500-26173, NREL, April 1999.
- [4] Hand, M., Simms, D., Fingersh, L., Jager, D., Cotrell, J., Schreck, S., and Larwood, S., "Unsteady Aerodynamics Experiment Phase VI: Wind Tunnel Test Configurations and Available Data Campaigns," Nrel/tp-500-29955, NREL, December 2001.
- [5] Sorensen NN, Michelsen JA, Schreck S. "Navier-stokes predictions of the NREL phase VI rotor in the NASA ames 80 ft 120 ft wind tunnel," Wind Energy 2002;2002(5):151-69.